Do rotating magnetic fields unconditionally lead to grain refinement? – A case study for directionally solidified Al-10wt%Cu alloys

Zimmermann, G.; Pickmann, C.; Schaberger-Zimmermann, E.; Galindo, V.; Eckert, K.; Eckert, S.;

Originally published:

August 2018

Materialia 3(2018), 326-337

DOI: https://doi.org/10.1016/j.mtla.2018.08.036

Perma-Link to Publication Repository of HZDR:

https://www.hzdr.de/publications/Publ-27860

Elsevier Editorial System(tm) for Acta Materialia

Manuscript Draft

Manuscript Number:

Title: Do rotating magnetic fields unconditionally lead to grain refinement? - A case study for directionally solidified Al-10wt%Cu alloys

Article Type: Full length article

Keywords: Aluminium-copper alloy; solidification; grain refinement, melt flow

Corresponding Author: Dr. Gerhard Zimmermann,

Corresponding Author's Institution:

First Author: Gerhard Zimmermann

Order of Authors: Gerhard Zimmermann; Christoph Pickmann; Elke Schaberger-Zimmermann; Vladimir Galindo; Kerstin Eckert; Sven Eckert

Abstract: The effect of solidification velocity and electromagnetic stirring on grain refining was investigated experimentally during the directional solidification of rod-like Al-10wt%Cu alloy samples. Applying low solidification velocities leads to a dendritic microstructure consisting of elongated equiaxed crystals, which result from fragmented dendrite arms forming new grains. This grain-refining effect vanishes for higher solidification velocities, leading to a microstructure dominated by a lower number of larger columnar grains. Moderate electromagnetic stirring under laminar flow conditions does not promote grain refinement. By contrast, a sufficiently strong forced melt flow induced by a rotating magnetic field significantly increases the number of grains in the range of solidification velocities investigated within this study. It is assumed that a turbulent melt flow supports the fragmentation of dendrite arms and thus the formation of new grains, which finally leads to grain refinement.

Suggested Reviewers: Andras Roosz
University of Miskolc
femroosz@uni-miskolc.hu
Expert in microstructure formation during solidification with melt flow

Petr A. Nikrityuk
University of Alberta at Edmonton
nikrityu@ualberta.ca
Expert of solidification modelling with melt flow

Yves Fautrelle
SIMAP, Grenoble
Yves.Fautrelle@simap.grenoble-inp.fr
Expert in solidification processing with external fields

Jonathan A. Dantzig

University of Illinois at Urbana-Champaign
dantzig@illinois.edu
Expert in microstructure formation and modelling of solidification

Henri Nguyen-Thi
IM2NP, Université Aix-Marseille
henri.nguyen-thi@im2np.fr
Expert in solidification experiments using Al-based alloys

access · Intzestraße 5 · 52072 Aachen · Germany

Prof. C. A. Schuh
Dept. of Materials Science and Engineering
Massachusetts Institute of Technology
77 Massachusetts Avenue, Cambridge, MA 02139
USA

our reference: GZ
direct dial: +49-241-80 98005
E.mail: g.zimmermann
@access-technology.de
Date: May 11, 2018

Submission to Acta Materialia

Dear Professor Schuh,

enclosed please find our manuscript entitled

Do rotating magnetic fields unconditionally lead to grain refinement? – A case study for directionally solidified Al-10wt%Cu alloys,

by G. Zimmermann, C. Pickmann, E. Schaberger-Zimmermann, V. Galindo, K. Eckert, and S. Eckert which we are submitting for publication in Acta Materialia.

Grain refinement by forced melt flow driven by electromagnetic fields is both of high technological relevance and of fundamental importance in solidification science. The dominating opinion in the solidification community, as documented in numerous research papers and reviews, is that the application of rotating magnetic fields always leads to a fine grained structure. However, a detailed understanding of the underlying mechanisms is missing. Does the forced flow lead to an enhanced remelting of secondary arms, which are able to promote grain growth afterwards? Or, is the forced flow responsible for the transport of dendrite fragments from the deeper mush zone?

One reason for the unsatisfying understanding of the interaction between dendritic growth and forced melt flow was the lack of possibilities of an in-situ visualization of the relevant processes on the microscale. This became possible only in the last years using X-ray visualization techniques.

Based on X-ray visualization we could recently clarify the fragmentation and the transport of secondary dendrite sidearms for an Al-10wt%Cu alloy, depending on the solidification velocity [Fragmentation-driven grain refinement in directional solidification of AlCu10wt-% alloy at low pulling speeds, Acta Materialia 126, 236-250, 2017]. For this particular composition, the initial melt composition and the solidifying primary Al dendrites have almost identical densities.

The main result of this study, which appeared surprising at first glance, is that equiaxed grain growth was found at low solidification velocities, instead of columnar growth. This exceptional behavior could be conclusively explained by the process of fragmentation. In-situ observation of the solidification process demonstrates that fragments continuously detach from the dendrite tip region and move slightly ahead of the solid-liquid interface as they grow. Due to the very small density difference between the fragment and the surrounding melt, the fragments were overgrown. As a result, an equiaxed grain structure appears at low solidification velocities, which is normally expected for much higher solidification velocities due to the classical columnar-to-equiaxed transition.

In the present manuscript we use this insights and understanding to apply a rotating magnetic field exactly at the same alloy system and configuration. By contrast to the opinion in the literature we show that the grain-refining effect of rotating magnetic fields behave non-monotonously: Without forced melt flow, equiaxed grain growth resulting from fragmentation was found at low solidification velocities. This grain-refining effect vanishes for higher solidification velocities, leading to a lower number of larger columnar grains. Intensive forced melt flow induced by a rotating magnetic field with a magnetic induction of B = 10 mT was found to significantly increase the number of grains throughout the range of solidification velocities investigated.

Thus we are able to show that the flow-induced grain-refinement effect only occurs when the flow intensity has exceeded a certain minimum value, likely associated with the transition from a laminar to a turbulent flow structure at the solidification front. Therefore, it can be assumed that only a turbulent melt flow supports the fragmentation of dendrite arms and thus the formation of new grains, which finally leads to grain refinement.

Hence, this study indicates that our understanding of the impact of electromagnetic stirring on solidification needs to be revised in several respects. We are confident that this thesis and the underlying results are of interest for the readers of Acta Materialia.

We are looking forward to your response,

Yours sincerely,
Access e.V.

Dr. Gerhard Zimmermann

Do rotating magnetic fields unconditionally lead to grain refinement? – A case study for directionally solidified Al-10wt%Cu alloys

G. Zimmermann[a,*], C. Pickmann[a], E. Schaberger-Zimmermann[b], V. Galindo[c], K. Eckert[c], S. Eckert[c]

[a] Access e.V, Intzestrasse 5, 52072 Aachen, Germany

[b] RWTH, Foundry Institute, Intzestrasse 5, 52072 Aachen, Germany

[c] HZDR, Institute of Fluid Dynamics, Bautzner Landstrasse 400, 01328 Dresden, Germany

[*] Corresponding author: Access e.V, Intzestrasse 5, 52072 Aachen, Germany,

Tel.: +49 241 8098005; Fax: +49 241 38578; email: g.zimmermann@access-technology.de

Abstract

The effect of solidification velocity and electromagnetic stirring on grain refining was investigated experimentally during the directional solidification of rod-like Al-10wt%Cu alloy samples. Applying low solidification velocities leads to a dendritic microstructure consisting of elongated equiaxed crystals, which result from fragmented dendrite arms forming new grains. This grain-refining effect vanishes for higher solidification velocities, leading to a microstructure dominated by a lower number of larger columnar grains. Moderate electromagnetic stirring under laminar flow conditions does not promote grain refinement. By contrast, a sufficiently strong forced melt flow induced by a rotating magnetic field significantly increases the number of grains in the range of solidification velocities investigated within this study. It is assumed that a turbulent melt flow supports the fragmentation of dendrite arms and thus the formation of new grains, which finally leads to grain refinement.

Keywords: Aluminium-copper alloy; solidification; grain refinement, melt flow

1. Introduction

Various techniques for achieving grain refinement during the solidification of metal alloys are widely used to improve the homogeneity of the cast microstructure. This can improve toughness, yield strength and formability [1]. For Al-based alloys, commercial grain-refiner particles such as Al–Ti or Al–Ti–B are often used to promote the formation of a fine, uniform, equiaxed grain structure during casting processes [2, 3]. Such potent nucleant particles are readily activated at a low level of undercooling to nucleate the primary phase [4]. The grain refinement strategy is particularly important for Al–Cu foundry alloys, which are very prone to hot tearing. It is well established that a sound grain-refining practice avoids hot tearing and allows a marked increase in casting speed [5].

AC magnetic fields unlock enormous potential to realize a variety of flow structures in molten metals, which makes electromagnetic stirring attractive for controlling the melt flow during solidification. Many studies have shown that beneficial effects can be obtained, such as distinct grain refinement or the promotion of a transition from columnar to equiaxed dendritic growth (CET) [6–10]. In particular, significant grain refinement was reported for electromagnetic stirring while applying rotating magnetic fields (RMFs) in Sn-Pb alloys [9], Al-based [11, 12], and Al-Cu alloys [13]. Campanella et al. used a pulsating magnetic field in Cu-based alloys and suggested a simple criterion for fragmentation induced by fluid flow on the basis of the partial remelting of dendrite arms [14]. The mechanism for grain refinement using melt convection is a subject of intensive debate. There is a general consensus in the point that the forced flow provokes an increase in the fragmentation rate. If there is a sufficiently large number of fragments, their growth is confined by their large number of direct neighbors, resulting in a fine structure of equiaxed grains.

Capillary effects cause pinch-off events in secondary dendrite arms during coarsening [15, 16] and are thus an important fragmentation mechanism. However, the dynamics of such processes are mainly determined by diffusive mass transfer, requiring long time scales. Convection accelerates the transport of solute and provokes distinct changes in the temperature and solute distribution within the solidifying melt. Intense convective transport of heat and solute in the mushy zone can lead the solid phase to partially remelt; in particular, side arm detachment may occur as a result of solute enrichment in the liquid between the dendrite arms [17–19]. Furthermore, the flow is supposed to subsequently transport the fragments into the undercooled regions adjacent to the solidification front, enabling the nucleation and growth of equiaxed grains [20]. Liotti et al. [21] investigated the effect of

forced convection on fragmentation in Al-Cu alloys by applying a pulsed magnetic field during solidification. They came to the general conclusion that intensifying the fluid flow leads to a higher fragmentation rate.

The objective of the present study is to examine the interaction of forced flow and fragmentation in greater depth. To this end, it continues a recent study on the directional solidification of Al-10wt%Cu alloy, where in-situ X-ray measurements at low solidification velocities determined that the fragmentation of dendrite arms was the dominant grain-refinement mechanism [22]. The fragments grow to a certain extent while forming finally an equiaxed grain structure. At higher solidification velocities, columnar dendritic growth is predominant and fragmentation is suppressed [23]. Fragmentation occurs in the upper region of the mushy zone. A temporary effect of buoyancy inside the Cu-rich solute boundary layer results in the separation of the fragments from the mushy zone and the growth of equiaxed crystals. Because the solidifying primary Al dendrites and the initial melt have almost the same values of density in Al-10wt%Cu alloy, the buoyant movement comes to rest at some distance from the mushy zone and the equiaxed crystals are caught up by the advancing solidification front.

On applying a rotating magnetic field to this configuration we want to address two questions: (i) Does the flow lead to a higher fragmentation rate? and (ii) Are the fragments transported by the flow ahead of the solidification front to stimulate equiaxed grain growth?

2. Experimental setup

The Al-Cu alloy used in the solidification experiments was prepared from high-purity Al and Cu. The samples were cast in rod-like steel moulds coated with boron nitride. The final composition measured by EDX analysis was Al-Cu with 10.0 wt% Cu. For directional solidification experiments, cylindrical samples with a diameter of D = 8 mm and a length of H = 200 mm were manufactured and integrated into alumina crucibles with an outer diameter of 10 mm. The experiments were carried out in a Bridgman-Stockbarger furnace with an argon atmosphere (**Fig. 1**). The temperature gradient was established between the cooling zone, i.e. a liquid metal bath at room temperature, and the heating zone, by means of an inductively heated graphite tube, separated by an insulating baffle. For the directional solidification experiments, the furnace was moved vertically along the sample (which was mounted in place) at a defined velocity. The experiments were performed with a constant temperature gradient of G = 10 K/mm. First, the samples were directionally melted and

thermally stabilized for about 10 min at the maximum melting position, then they were directionally solidified by constant furnace velocities in the range between 8.3 µm/s and 167 µm/s.

The gradient furnace was equipped with a rotating magnetic field (RMF) device. The height of the three coil pairs is 100 mm, allowing for a homogeneous magnetic induction of the same extent inside the sample. The coil system was moved together with the furnace. It was positioned close to the solid-liquid interface region of the samples and the melt region ahead. The frequency of the RMF was fixed at f = 50 Hz and the magnetic induction could be varied continuously between B = 0 and B = 13 mT. This determined the intensity of the induced melt flow. For the experiments shown here, magnetic inductions of B = 0, B = 2 mT and B = 10 mT were applied to realize experimental conditions where the solidification process occurs without induced flow, or is affected by moderate and intense forced flows, respectively.

To analyze the microstructure and the grain structure in the processed samples, longitudinal and radial cross-sections were prepared for steady-state solidification conditions. The dendritic microstructure and the radial segregation due to the RMF were determined from polished radial cross-sections of the bulk samples. Then, electrolytically etched cross-sections were investigated in a polarization microscope to show grains with different crystallographic orientations in different colors and therefore to allow the grain structure to be analyzed [24].

3. Results

3.1 Microstructure and radial segregation

The Al-10.0 wt-%Cu samples were directionally solidified in a temperature gradient of G = 10 K/mm with furnace movements V of 8.3 µm/s and 16.7 µm/s, 33.3 µm/s, 41.7 µm/s, 83.3 µm/s and 167 µm/s, and RMF induction B of 0 mT, 2 mT and 10 mT.

The microstructures in the radial cross-sections for three solidification velocities are presented in **Fig. 2**. The microstructures without forced melt flow (B = 0 mT) and with forced melt flow (B = 10 mT) are compared in the left and in the right column, respectively. The main observation is that the intense melt flow results in an accumulation of eutectic fraction in the center of the sample, which was more pronounced at low solidification velocities. To quantify this radial segregation, concentration measurements were performed in a scanning electron microscope using an EDX device. **Fig. 3** shows the radial concentration profiles of Cu in

samples solidified with $V = 41.7$ µm/s, but under the influence of different magnetic inductions B. For the highest value, $B = 10$ mT, a distinct increase was measured in the Cu content in the center region, up to about 15 wt%.

3.2 Grain structure

To analyze the grain structure in the processed bulk samples, both radial and longitudinal cross-sections were electrolytically etched and viewed in a polarization microscope. **Fig. 4** shows the results for the Al-10wt%Cu alloy solidified by applying a temperature gradient of $G = 10$ K/mm and 4 different solidification velocities V. The magnetic induction B was varied in three steps and comprised solidification without forced convection, and under the influence of weak and intense electromagnetic stirring, respectively.

The average number of grains N and the average grain size A_{Gr} were determined by evaluating the radial cross-sections. Therefore, in a first step the grain structure was automatically reconstructed by distinguishing the individual grains using different colors. In some cases, it was found that there were grain areas of nearly uniform color, which, upon closer inspection, consisted of subregions of dendrites which had different orientations with respect to their axis. In these cases, in a second step, such sub-areas were manually identified as separate grains. As a result, the grain structure obtained with delineated contour lines is presented in **Fig. 4**. Two main tendencies became obvious. Firstly, the number of grains increases as the solidification velocities decrease for all variations on the flow conditions considered here. Secondly, intensive stirring applying a magnetic field of $B = 10$ mT clearly increases the number of grains, whereas this effect is not observed with the lower magnetic field of $B = 2$ mT. On the contrary, the impression is created that significantly fewer grains even occur, especially at higher solidification velocities.

Fig. 4a shows the microstructures resulting from the solidification at the lowest solidification velocity of $V = 16.7$ µm/s, Inspecting the longitudinal cross sections reveals a prevailing equiaxed grain structure both without forced convection and with intensive electromagnetic stirring. A previous study, which dealt with the reference case without forced convection, demonstrated that the occurrence of equiaxed grains can be conclusively explained by the process of fragmentation [22, 25]. Small equiaxed grains are also observable in the case of weak convection ($B = 2$ mT), but here the vast majority of the area is covered by several larger columnar grains. Such extended columnar grains disappear at the higher magnetic field, while many small equiaxed grains emerge. In the case of larger grains, it is difficult to decide

whether they can still be classified as columnar grains or as elongated equiaxed grains. In contrast to the microstructure at $B = 2$ mT, where the columnar grains apparently grow parallel to the temperature gradient, the orientation of the elongated grains at $B = 10$ mT is inclined with respect to the axis of the cylindrical sample. For higher solidification velocities, the grain size continuously increases and the grain structure consists of a few large, mainly axially oriented columnar grains and some grains which are misoriented, the latter being observed in appreciable numbers only in the case of intensive stirring (see **Fig. 4b-d**).

The average grain size is determined as the mean value of all grain areas detected in a cross-section. To check the reproducibility of the grain structure, several samples were solidified using the same experimental parameters. The grain structure analysis demonstrates that the variations in N and A_{Gr} are less than 10%.

The evaluation results in **Fig. 5** show that in the case without a forced melt flow ($B = 0$ mT), there are a large number of small grains at low solidification velocities, while the corresponding number of grains in the intensively stirred samples is larger by almost a factor of two. An increase in the solidification rate causes a significant decrease in the number of grains for all three cases studied, the intensively stirred samples always having a distinctly higher number of grains with correspondingly smaller grain size. A very interesting finding is the fact that, at high solidification velocities, weakly stirred samples ($B = 2$ mT) actually contain measurably fewer grains than in the reference case without a magnetic field.

4. Discussion

The starting point of the current study was the recent finding that fragmentation leads to the formation of equiaxed grains in directionally solidified Al-10wt%Cu alloys at low solidification velocities [22]. In-situ observation of the solidification process obtained by X-ray radiography demonstrated that fragments continuously detach from the dendrites in the zone near the tip. Within the concentration boundary layer, these fragments are moved slightly ahead of the solid-liquid interface by buoyancy while they grow. Due to the very small density difference between the fragment and the surrounding melt, this movement comes to a standstill after path lengths of the order of 1 mm, and the fragments were overgrown. As a result, an equiaxed grain structure appears at low solidification velocities.

With this aspect well understood, the question arises of what influence a forced flow, driven by an RMF in the solidifying melt, has on this process? The exposure of an RMF to a metal alloy in a cylindrical column leads to a primary, swirling azimuthal motion of the liquid and a

secondary, recirculating flow in the r-z plane resulting from the Ekman pumping at the horizontal walls [26-29]. In our case, the secondary vortices are mainly driven by the axial pressure drop at the bottom. The intensity of the melt flow can be assessed using the non-dimensional magnetic Taylor number Ta_m,

$$Ta_m = \frac{B^2 \cdot R^4 \cdot \sigma \cdot \pi \cdot f}{\rho \cdot \nu^2} \qquad (1)$$

where B denotes the amplitude of the magnetic field, R the sample radius, σ the electrical conductivity of the melt, f the rotational frequency of the magnet, ρ the density of the melt and ν the kinematic viscosity. In the experiments, the intensity of the induced melt flow was controlled by varying the magnetic induction B. Inserting the respective parameters and the material properties of Al-10wt%Cu [30] into equation (1) results in magnetic Taylor numbers of $Ta_m = 1220$ and $Ta_m = 30500$ for $B = 2$ mT and $B = 10$ mT, respectively. The critical value for a transition from a laminar to a turbulent flow in a finite circular cylinder of aspect ratio 1 is $Ta_{m,cr} = 1.23\times10^5$ [31]. Below the critical value of the magnetic Taylor number $Ta_{m,cr}$, the RMF-driven flow remains laminar and steady. However, the higher the cylinder is, the faster the RMF flow becomes unstable, i.e. the critical Taylor number decreases as the aspect ratio H/D increases. Grants & Gerbeth [31] found a critical Taylor number of 0.22×10^5 for an aspect ratio of 2, while Nikrityuk et al. [32] showed a further decrease to 0.07×10^5 for an aspect ratio of 4.

The flow in the volume containing the melt was simulated numerically by solving the Navier–Stokes equation (momentum conservation) together with the incompressibility condition div(v)=0 and using the finite volume library OpenFOAM. The time-averaged electromagnetic induced force density in the melt was taken into account by adding a body force to the momentum equation. For the electromagnetic force density, an analytical expression can be given in the low-frequency and low-induction approximation [33] which has an azimuthal component only. Due to the expected low value of the Taylor number, we assumed the flow structure to be axisymmetric. For the simulations in the case considered here, a fluid height of 100 mm and thus an aspect ratio of 12.5 were assumed. For this aspect ratio, we have no accurate information about the stability limit, but our calculations show that the flow at $B = 2$ mT is still laminar, while a turbulent flow occurs at $B = 10$ mT.

A characteristic melt flow pattern is shown in **Fig. 6a**. The sketch shows the primary azimuthal flow and the secondary radial flow close to the solid-liquid interface [27]. The flow velocity of this secondary flow is typically less than 20% of that of the primary azimuthal flow, see Fig. 3 in [32]. However, this convection roll transports mass ahead and inside the

mushy zone from the outer part to the centre. This flow is responsible for the Cu enrichment in the centre of the samples at B = 10 mT (see Fig. 3). As a result, this radial segregation leads to an increase in the eutectic fraction there (see Fig. 2). This effect is more significant for low solidification velocities. In the case of higher solidification velocities, the time interval for mass transport by the secondary radial flow is shorter, resulting in less segregation.

Fig. 6b presents the calculated contour maps of all three velocity components u_r, u_z and u_φ for a magnetic induction of B = 2 mT, while Figs. 6c and d show the corresponding velocity profiles along the radius at distances of 1 mm and 0.5 mm from the bottom, respectively. It becomes obvious that the maximum values of all three components are about one order of magnitude larger than the solidification velocities applied within this study. This surprising finding, that the moderate stirring does not have any consequences with regard to an increase in equiaxed crystals in the microstructure, actually contradicts the common opinion. For instance, a simple criterion was suggested in the literature indicating that flow-induced local remelting could occur when the component of the fluid flow velocity along the thermal gradient becomes larger than the velocity of the isotherms [14]. Although in our case the primary flow direction is perpendicular to the temperature gradient, even the vertical component of the secondary flow clearly exceeds the pull rate. Nevertheless, no fragmentation is observed; rather, a decline in the grain number is seen at higher solidification rates. In fact, it is assumed that melt convection contributes significantly to fragmentation when transporting solute-enriched fluid to the mushy zone, or inducing considerable fluctuations in concentration and / or temperature in the immediate vicinity of the dendrites. Moreover, the transport of fragments from the mushy zone into areas just before the solidification front and the removal of the latent heat should promote equiaxed growth.

But, at least in the case of an RMF-driven flow, these effects obviously only become effective at significantly higher fluid velocities. Indeed, for the directional solidification of Pb-Sn alloys, it has been observed that the application of an RMF causes grain refinement and promotes the columnar-to-equiaxed transition (CET) at Ta numbers above 10^6 [34]. The effect of forced convection on the solidification of Ga-In alloys was investigated using X-ray radiography [35]. Similarly to the present study, in these experiments the forced flow generated by a magnetic pump was also mainly perpendicular with respect to the growth direction and greater than the progression of the solidification front by a factor of 10. In-situ visualization revealed that the forced flow eliminates buoyant plumes of solute and damps local fluctuations in the concentration. As a result, the dendrite side arms were observed to

develop unevenly with respect to their orientation to the flow direction, but no noticeable increase was seen in the fragmentation rate.

Furthermore, the local flow structure around the dendrite tips, and hence also the solute boundary layer, are strongly determined by the roughness of the growing front. A basically unstable density distribution due to a lateral incident flow along a rough solidification front is observed in the X-ray visualization of a solidifying Ga-25wt%In alloy [36], see **Fig. 7**. Here, the forced flow obviously suppresses substantial convective transport in the vertical direction. Recirculation areas develop behind the dendrites, retaining the less dense solute-rich liquid within the interdendritic zones.

Taking all these observations into account, the stabilization of columnar growth during moderate electromagnetic stirring can be explained as follows: the horizontal flow along the solidification front primarily leads to a considerable reduction in the solutal boundary layers. This effect restricts the driving buoyancy force to a small zone around the dendrites. This force is necessary to move the fragments into the area directly in front of the columnar dendrite tips, where they can form equiaxed grains. Since this force is weak in the present case, it is likely that the laminar flow leads to the fragments being trapped in the recirculation vortices, which appear in the flow behind the dendrites, schematically shown by arrows in **Fig. 7**. A turbulent flow is obviously needed to release the fragments from the recirculation vortices into the subcooled zone ahead of the solidification front. Indeed, with a turbulent flow two further processes come into play. First, fluctuating convective transport of concentration can lead to the additional formation of fragments. Second, the flow around the dendrites generates a turbulent wake characterized by a repetitive detachment of single vortices. This detachment is associated with the local occurrence of significant ascending flow, which can eject the fragments from the mushy zone. Consequently, in the case of strong stirring (B = 10 mT), a significant increase in equiaxed grains is observed (see **Fig. 4**).

Moreover, the azimuthal melt flow at B = 10 mT results in grains bending, as shown by the electro-oxidized microstructure given in **Fig. 4**. In **Fig. 8** the location of the longitudinal cross-sections in the solidified Al-10wt%Cu sample is shown together with a schematic of the azimuthal flow field u_φ in a horizontal plane. At the positions of the longitudinal cross-sections, somewhat offset from the centre of the sample, the azimuthal flow throughout the longitudinal cross-section always features a resulting lateral component $u_{\varphi,res}$. With respect to the rotating direction of the melt, the grains grow towards the primary azimuthal flow [37, 38]. This can be explained by the convective transport of solute rejected from the vicinity of the columnar front into the bulk region of the melt, leading to a steeper concentration gradient

on the upstream side as well as in front of the dendrite tips. The corresponding enhancement of the constitutional undercooling triggers a growth in the dendritic structure towards the flow direction [37].

5. Conclusions

The directional solidification behavior of Al-10wt%Cu alloy was investigated experimentally in rod-like samples. Without forced melt flow, equiaxed grain growth resulting from fragmentation was found at low solidification velocities. This grain-refining effect vanishes for higher solidification velocities, leading to a lower number of larger columnar grains.

Intensive forced melt flow induced by a rotating magnetic field with a magnetic induction of $B = 10$ mT was found to significantly increase the number of grains throughout the range of solidification velocities investigated. It can be assumed that fragmented dendrite arms were transported by the melt flow and act as nuclei for new grains. Thus, forced melt flow led to a considerable grain refinement in Al-10wt%Cu alloy.

However, this study also shows that the flow-induced grain-refinement effect only occurs when the flow intensity has exceeded a certain minimum value, likely associated with the transition from a laminar to a turbulent flow structure at the solidification front. This is impressively substantiated by the fact that moderate stirring at $B = 2$ mT does not lead to any grain refinement but even causes a decrease in the number of grains. A sufficiently strong but laminar lateral flow along the dendritic front reduces the thickness of the solutal boundary layer and inhibits flow components perpendicular to the solidification front. It is unlikely that fragments formed under these circumstances during the solidification of the Al-10wt%Cu alloy will be able to reach the area of constitutional supercooling ahead of the tips of the columnar dendrites, where they can develop into equiaxed grains. Hence, this study indicates that our understanding of the impact of electromagnetic stirring on solidification needs to be revised in several respects. Given that the turbulent properties of the forced convection appear to play an essential role in promoting grain refinement, further investigations will be needed to better understand the complex interaction between solidification and melt flow.

Acknowledgements

Financial support by the Helmholtz Association as part of the Helmholtz Alliance LIMTECH is gratefully acknowledged. We thank Dres. N. Shevchenko and O. Keplinger for fruitful discussions on fluid flow impact during the solidification of Ga-In alloys.

References

[1] J.A. Spittle, Grain refinement in shape casting of aluminium alloys, International Journal of Cast Metals Research 19 (2006) 210–222.

[2] A.L. Greer, P.S. Cooper, M.W. Meredith, W. Schneider, P. Schumacher, J.A. Spittle, A. Tronche, Grain refinement of aluminium alloys by inoculation, Adv. Eng. Mater. 5 (2003) 81–91.

[3] P.S. Mohanty, J.E. Gruzleski, Mechanism of grain refinement in aluminium, Acta Metall. Mater. 43 (1995) 2001–2012.

[4] B.S. Murty, S.A. Kori, M. Chakraborty, Grain refinement of aluminium and its alloys by heterogeneous nucleation and alloying, International Materials Reviews 47 (2002) 3–29.

[5] Y. Birol, Grain refinement of Al–Cu foundry alloys with B additions, International Journal of Cast Metals Research 25 (2012) 117–120.

[6] C. Vives, Hydrodynamic, thermal and crystallographical effects of an electromagnetically driven rotating flow in solidifying aluminium alloy melts, Int. J. Heat Mass Transfer 33 (1990) 2585–2598.

[7] W.D. Griffiths, D.G. McCartney, The effect of electromagnetic stirring during solidification on the structure of Al_Si alloys, Mater. Sci. Eng. A 216 (1996) 47–60.

[8] J.K. Roplekar, J.A. Dantzig, A study of solidification with a rotating magnetic field, Int. J. of Cast Metals Research 14 (2001) 79–95.

[9] B. Willers, S. Eckert, U. Michel, I. Haase, G. Zouhar, The columnar-to-equiaxed transition in Pb-Sn alloys affected by electromagnetically driven convection, Mater. Sci. Eng. A 402 (2005) 55–65.

[10] S. Eckert, P.A. Nikrityuk, B. Willers, D. Räbiger, N. Shevchenko, H. Neumann-Heyme, V. Travnikov, S. Odenbach, A.Voigt, K. Eckert, Electromagnetic melt flow control during solidification of metallic alloys, The European Physical Journal – Special Topics 220 (2013), 123–137.

[11] B. Fragoso, H. Santos, Effect of a rotating magnetic field at the microstructure of an A354, Journal of Materials Research and Technology 2(2) (2013) 100–109.

[12] B. Willers, S. Eckert, P.A. Nikrityuk, D. Räbiger, J. Dong, K. Eckert, G. Gerbeth, Efficient melt stirring using pulse sequences of a rotating magnetic field: Part II.

Application to solidification of Al-Si alloys, Metallurgical and Materials Transactions B 39 (2) (2008), 304–316.

[13] H. Wei, F. Xia, S. Qian, M. Wang, Effect of permanent magnetic stirring on the solidification microstructure and ingot quality of Al-Cu alloys, Journal of Materials Processing Technology 240 (2017) 344–353.

[14] T. Campanella, C. Charbon, M. Rappaz, Grain refinement induced by electromagnetic stirring: A dendrite fragmentation criterion, Metall Mater Trans A35(10) (2004) 3201–3210.

[15] H. Neumann-Heyme, K. Eckert, C. Beckermann, Dendrite fragmentation in alloy solidification due to sidearm pinch-off, Phys. Rev. E 92 (2015) 060401(R)

[16] H. Neumann-Heyme, S. Shevchenko, Z. Lei, K. Eckert, O. Keplinger, J. Grenzer, C. Beckermann, S. Eckert, Coarsening evolution of dendritic sidearms: from synchrotron experiments to quantitative modelling, Acta Mater. 146 (2018) 176–186.

[17] K.A. Jackson, J.D. Hunt, D.R. Uhlmann, T.P. Seward, On the origin of the equiaxed zone in castings, Trans. Met. Soc. AIME 236 (1966) 149–158.

[18] D. Ruvalcaba, R.H. Mathiesen, D.G. Eskin, L. Arnberg, L. Katgerman, In situ observations of dendritic fragmentation due to local solute-enrichment during directional solidification of an aluminum alloy, Acta Mater. 55 (2007) 4287–4292.

[19] H. Jung, N. Mangelinck-Noel, H. Nguyen-Thi, N. Bergeon, B. Billia, A. Buffet, G. Reinhart, T. Schenk, J. Baruchel, Fragmentation in an Al–7 wt-%Si alloy studied in real time by X-ray synchrotron techniques, Int. J. Cast Metals Res. 22 (2009) 208–211.

[20] A. Hellawell, S. Liu, S.Z. Lu, Dendrite fragmentation and the effects of fluid flow in castings, JOM 49 (1997) 18–20.

[21] E. Liotti, A. Lui, S. Kumar, Z. Guo, C. Bi, T. Connolley, P.S. Grant, The spatial and temporal distribution of dendrite fragmentation in solidifying Al-Cu alloys under different conditions, Acta Mater. 121 (2016) 384–395.

[22] G. Zimmermann, C. Pickmann, M. Hamacher, E. Schaberger-Zimmermann, H. Neumann-Heyme, K. Eckert, S. Eckert, Fragmentation-driven grain refinement in directional solidification of AlCu10wt-% alloy at low pulling speeds, Acta Materialia 126 (2017) 236–250.

[23] G. Zimmermann, C. Pickmann, E. Schaberger-Zimmermann, K. Eckert, S. Eckert, Fragmentation in directionally solidified Al-10wt%Cu alloy at low pulling speeds, Proc. of the 6th Decennial International Conference on Solidification Processes (2017) 120–123.

[24] E. Schaberger, F. Grote, A. Schievenbusch, Farbätzung und Farbbildanalyse: Ein Weg zur Charakterisierung von Gefügen innovativer Gusswerkstoffe, Prakt. Metallographie 37 (2000) 419–434.

[25] N. Shevchenko, H. Neumann-Heyme, C. Pickmann, E. Schaberger-Zimmermann, G. Zimmermann, K. Eckert, S. Eckert, Investigations of fluid flow effects on dendritic solidification: Consequences on fragmentation, macrosegregation and the influence of electromagnetic stirring, IOP Conf. Series: Materials Science and Engineering 228 (2017) 012005 doi:10.1088/1757-899X/228/1/012005

[26] P. A. Davidson, The interaction between swirling and recirculating velocity components in unsteady inviscid flow, Journal of Fluid Mechanics 209 (1989) 35–55.

[27] G. Zimmermann, L. Sturz, M. Walterfang, J. Dagner, Effect of melt flow on dendritic growth in AlSi7-based alloy during directional solidification, International Journal of Cast Metals Research 22(1–4) (2009) 335–338.

[28] A. Noeppel, A. Ciobanas, X.D. Wang, K. Zaidat, N. Mangelinck, R. Moreau, A. Weiss, G. Zimmermann, Y. Fautrelle, Influence of forced/natural convection on segregation during the directional solidification of Al-based binary alloys, Metall. Mater. Transact. B41 (2010) 193-208.

[29] A. Roósz, A. Rónaföldi, J. Kovács, M. Svéda, Effect of low rotating magnetic field (RMF) induced melt flow on the microstructure of unidirectionally solidified Al-7wt.%Si-1wt.%Fe Alloy, Proc. of the 6th Decennial International Conference on Solidification Processes (2017) 308–311.

[30] Y. Plevachuk, V. Sklyarchuk, A. Yakymovych, S. Eckert, B. Willers, K. Eigenfeld, Density, Viscosity, and Electrical Conductivity of Hypoeutectic Al-Cu Liquid Alloys, Metallurgical and Materials Transactions A 39 (2008) 3040–3045.

[31] I. Grants, G. Gerbeth, Linear three-dimensional instability of a magnetically driven rotating flow, Journal of Fluid Mechanics 463 (2002) 229–239.

[32] P. A. Nikrityuk, K. Eckert, R. Grundmann, Numerical study of a laminar melt flow driven by a rotating magnetic field in enclosed cylinders with different aspect ratios, Acta Mechanica 186 (2006) 17–35

[33] L. P. Gorbachev, N. V. Nikitin, A. L. Ustinov, Magnetohydrodynamic rotation of an electrically conductive liquid in a cylindrical vessel of finite dimensions, Magnetohydrodynamics 10 (1974) 406–414.

[34] B. Willers, S. Eckert, U. Michel, I. Haase, G. Zouhar, The columnar-to-equiaxed transition in Pb-Sn alloys affected by electromagnetically driven convection, Materials Science Engineering A 402 (2005) 55–65.

[35] N. Shevchenko, O. Roshchupkina, O. Sokolova, S. Eckert, The effect of natural and forced convection on dendritic solidification in Ga-In alloys, Journal of Crystal Growth 417 (2015) 1–8.

[36] O. Keplinger, N. Shevchenko, S. Eckert: unpublished data (2018)

[37] S. Eckert, D. Räbiger, G. Zimmermann, E. Schaberger-Zimmermann, M. Mathes, The impact of melt flow on the grain orientation in solidifying metal alloys, ICASP-3; IOP Conference Series: Materials Science and Engineering 27 (2011) 012051

[38] A.N. Turchin, D.G. Eskin, L. Katgerman, Effect of melt flow on macro- and microstructure evolution during solidification of an Al–4.5% Cu alloy, Mater. Sci. Eng. A413–414 (2005) 98–104.

Figure captions:

Fig. 1: a) Bridgman-Stockbarger furnace with rotating magnetic field (RMF) and b) sketch of the set-up

Fig. 2: Microstructure in radial cross-sections of Al-10wt%Cu alloy (G = 10 K/mm) solidified with different velocities V; left column: without forced melt flow (B = 0 mT), right-hand column: with forced melt flow (B = 10 mT)

Fig. 3 Radial profiles of Cu concentration in samples solidified with V = 41.7 µm/s, but with different magnetic induction B.

Fig. 4a: Grain structure in radial (top) and longitudinal cross-sections of Al-10wt%Cu alloy solidified with G = 10 K/mm, V = 16.7 µm/s and with 3 different magnetic induction B

Fig. 4b: Grain structure in radial (top) and longitudinal cross-sections of Al-10wt%Cu alloy solidified with G = 10 K/mm, V = 41.7 µm/s and with 3 different magnetic induction B

Fig. 4c: Grain structure in radial (top) and longitudinal cross-sections of Al-10wt%Cu alloy solidified with G = 10 K/mm, V = 83.3 µm/s and with 3 different magnetic induction B

Fig. 4d: Grain structure in radial (top) and longitudinal cross-sections of Al-10wt%Cu alloy solidified with G = 10 K/mm, V = 166.7 µm/s and with 3 different magnetic induction B

Fig. 5: Average number of grains N (top) and average grain size A_{gr} (bottom) for different solidification velocities V and different magnetic induction B with trend lines for better allocation

Fig. 6: a) Sketch of the flow structures induced by an RMF consisting of a primary azimuthal flow and a secondary meridional flow, b) calculated distributions of all velocity components for a magnetic induction of B = 2 mT, and velocity profiles at distances from the bottom of c) 1 mm and d) 0.5 mm.

Fig. 7: X-ray visualization of directional solidification in Ga-25wt%In alloy under the effect of an incident lateral melt flow produced by a magnetic pump [34]. The colors represent the local composition of both the solid and the liquid phase (blue – In dendrites, red – Ga-rich liquid). The blue arrows mark the flow direction.

Fig. 8: Location of the longitudinal cross-section in the solidified Al-10wt%Cu sample with schematic azimuthal flow field u_φ in a horizontal plane and the lateral component $u_{\varphi,res}$ in the longitudinal cross-section

Figure 1

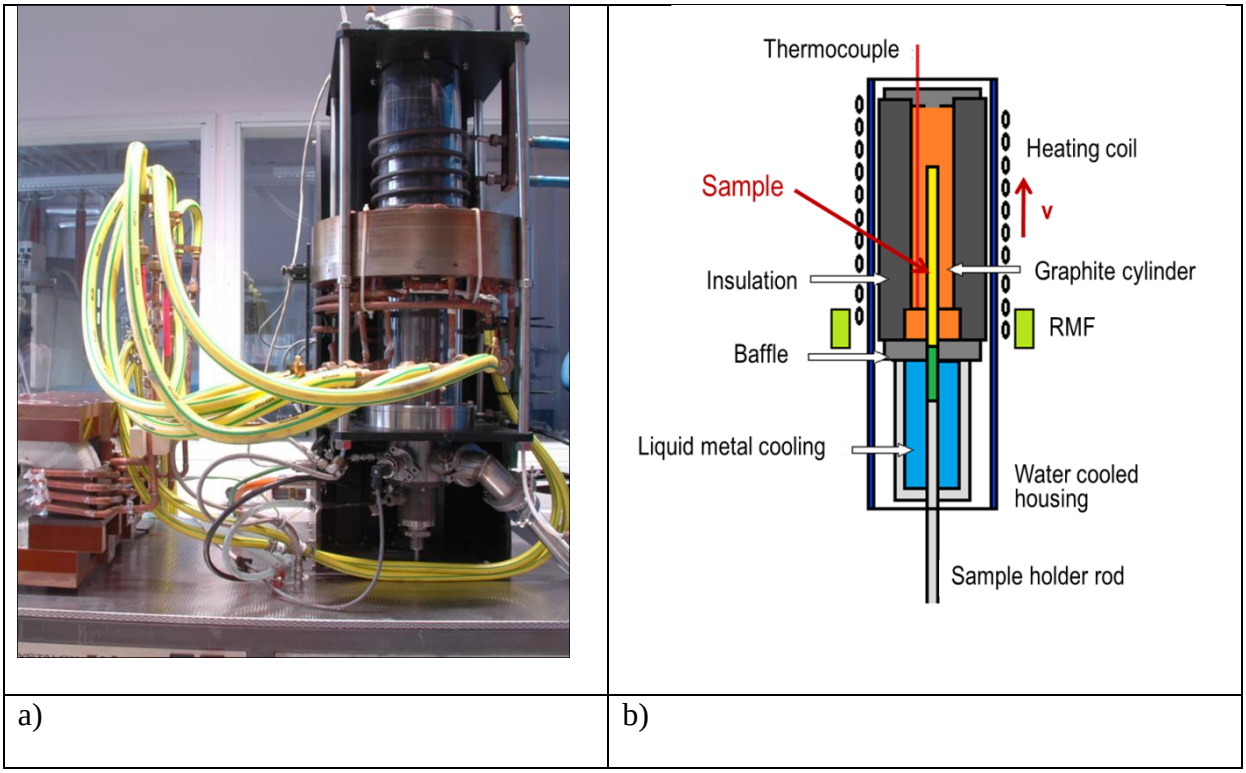

a) b)

Fig. 1: a) Bridgman-Stockbarger furnace with rotating magnetic field (RMF) and b) sketch of the set-up

Figure 2

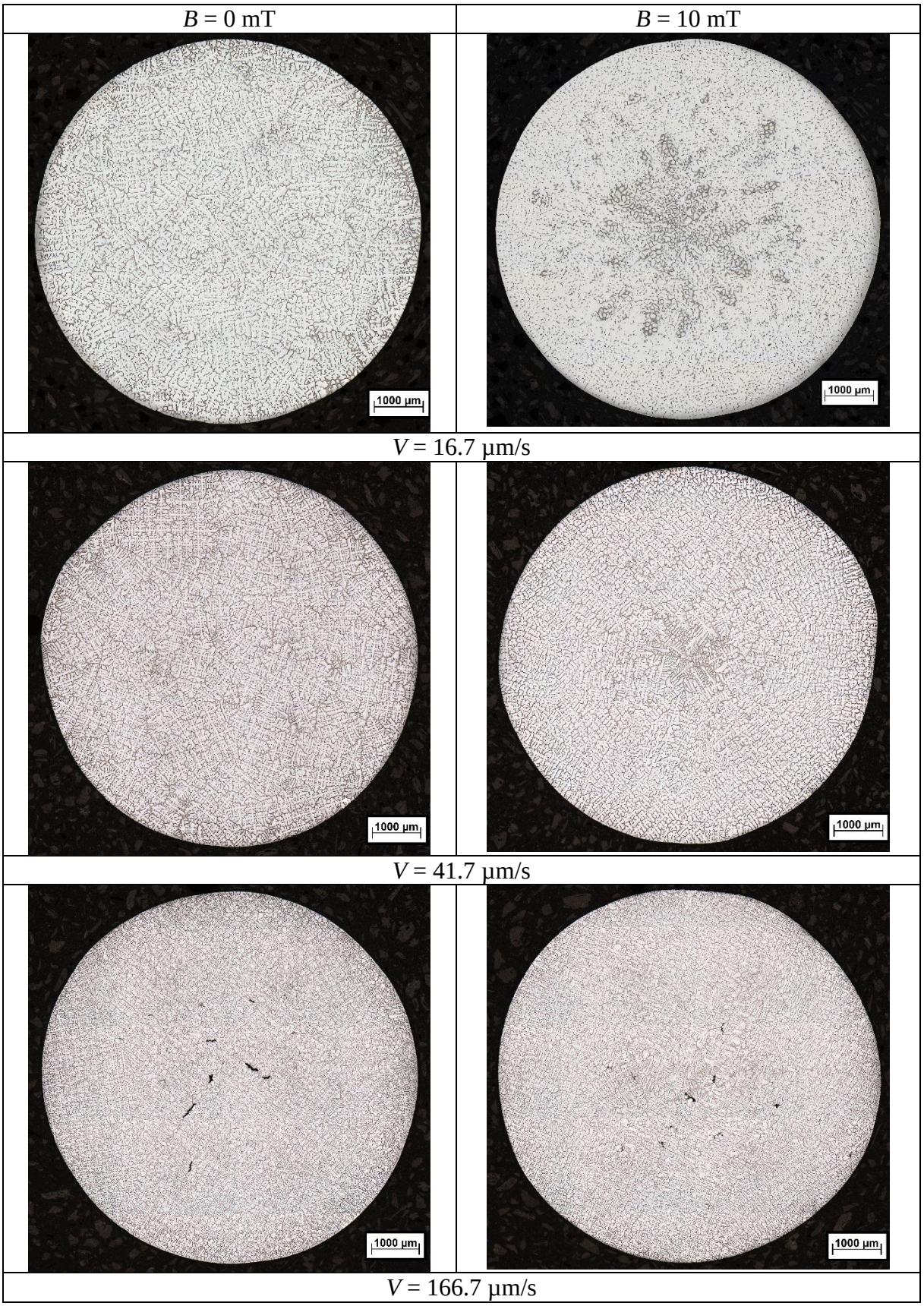

Fig. 2: Microstructure in radial cross-sections of Al-10wt%Cu alloy (G = 10 K/mm) solidified with different velocities V; left column: without forced melt flow (B = 0 mT), right-hand column: with forced melt flow (B = 10 mT)

Figure 3

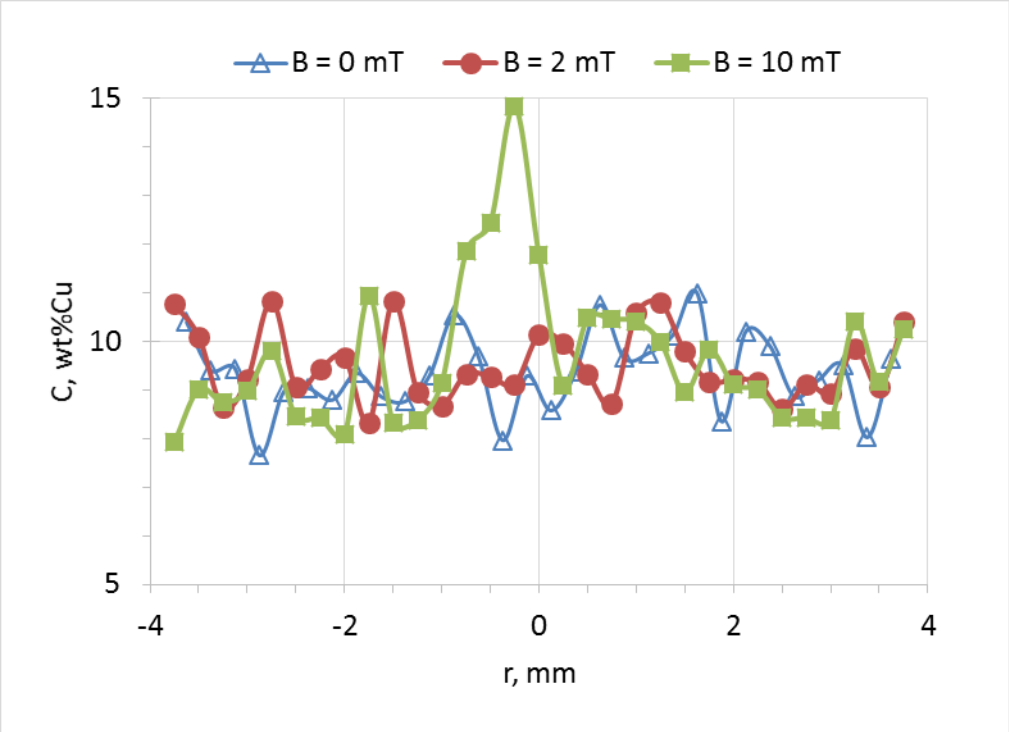

Fig. 3 Radial profiles of Cu concentration in samples solidified with $V = 41.7$ μm/s, but with different magnetic induction B.

Figure 4a

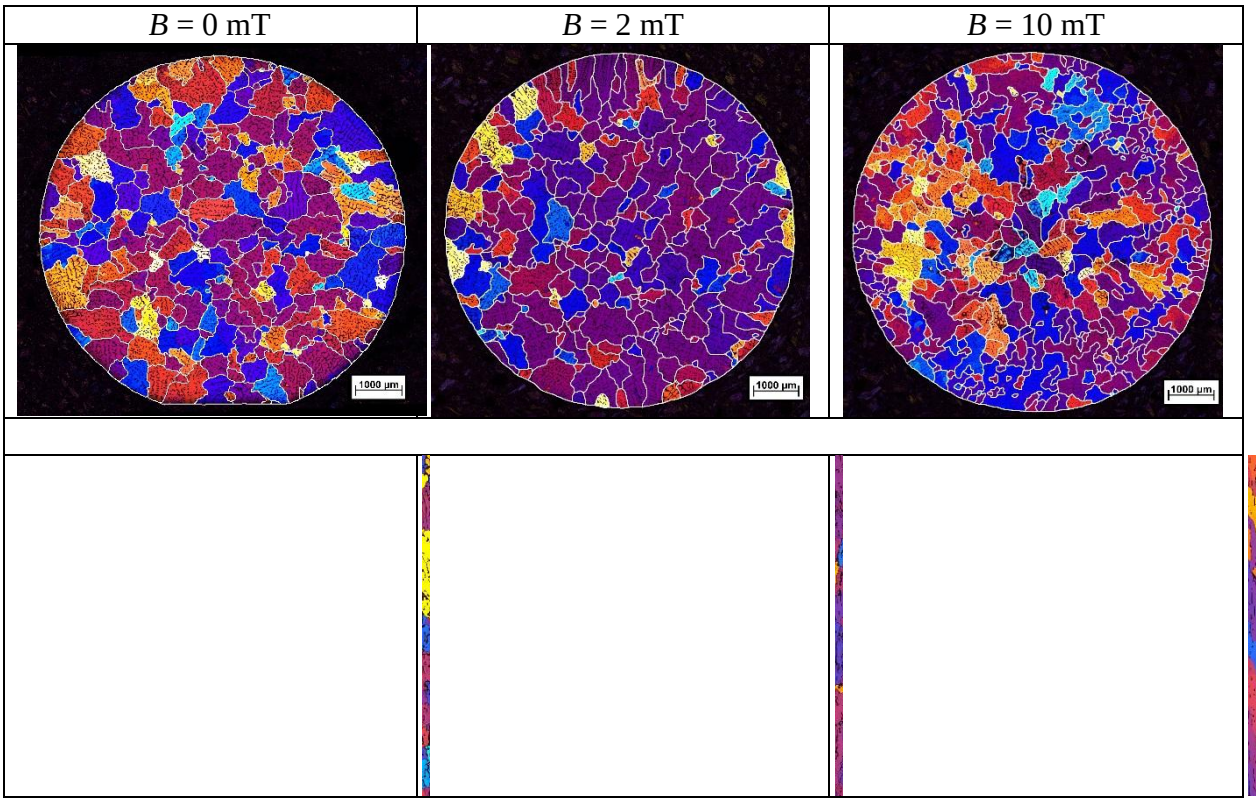

Fig. 4a: Grain structure in radial (top) and longitudinal cross-sections of Al-10wt%Cu alloy solidified with G = 10 K/mm, V = 16.7 µm/s and with 3 different magnetic induction B

Figure 4b

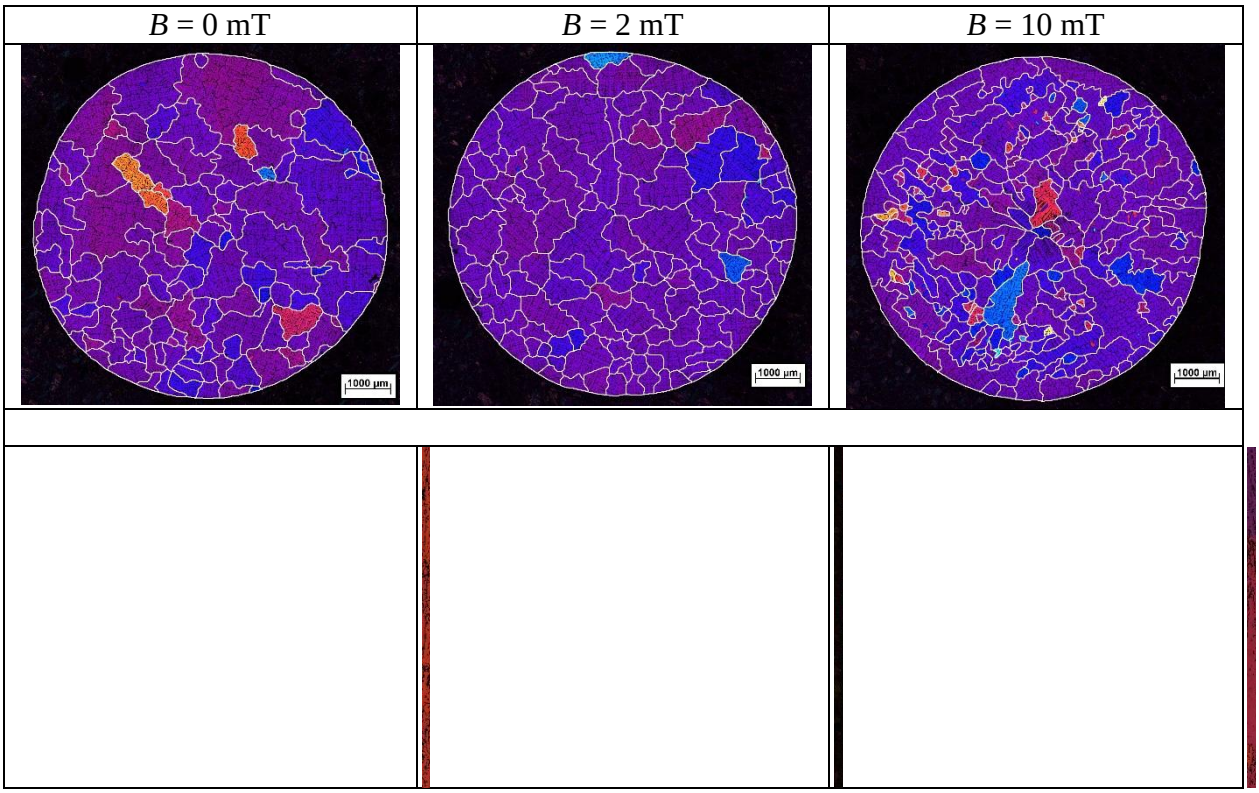

Fig. 4b: Grain structure in radial (top) and longitudinal cross-sections of Al-10wt%Cu alloy solidified with G = 10 K/mm, V = 41.7 µm/s and with 3 different magnetic induction B

Figure 4c

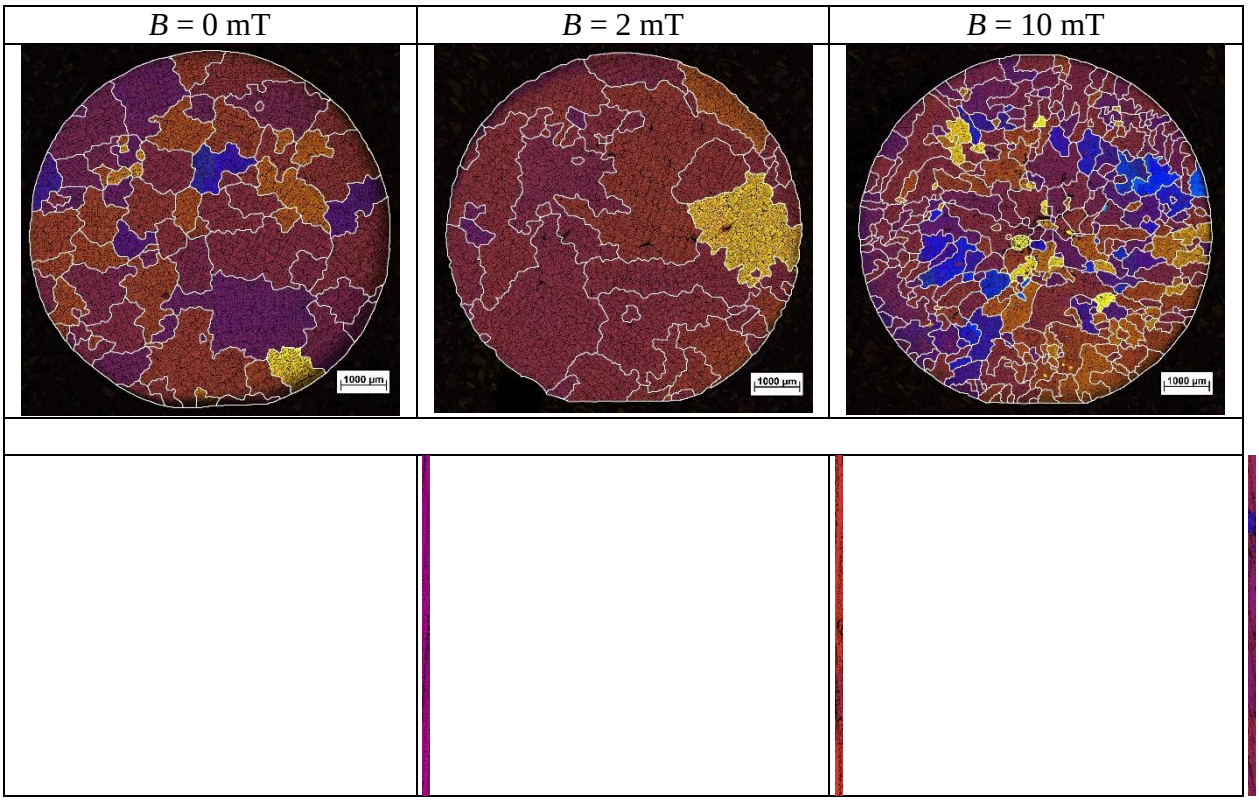

Fig. 4c: Grain structure in radial (top) and longitudinal cross-sections of Al-10wt%Cu alloy solidified with G = 10 K/mm, V = 83.3 µm/s and with 3 different magnetic induction B

Figure 4d

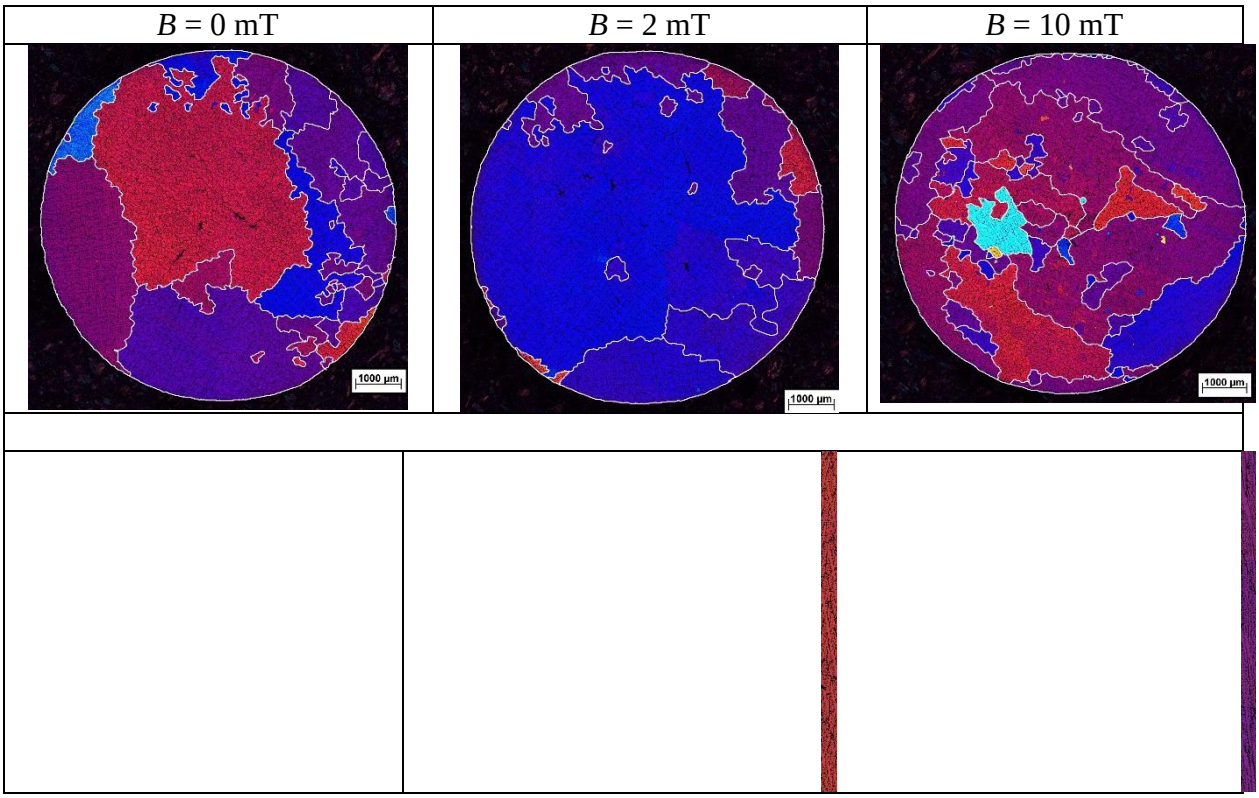

Fig. 4d: Grain structure in radial (top) and longitudinal cross-sections of Al-10wt%Cu alloy solidified with G = 10 K/mm, V = 166.7 µm/s and with 3 different magnetic induction B

Figure 5

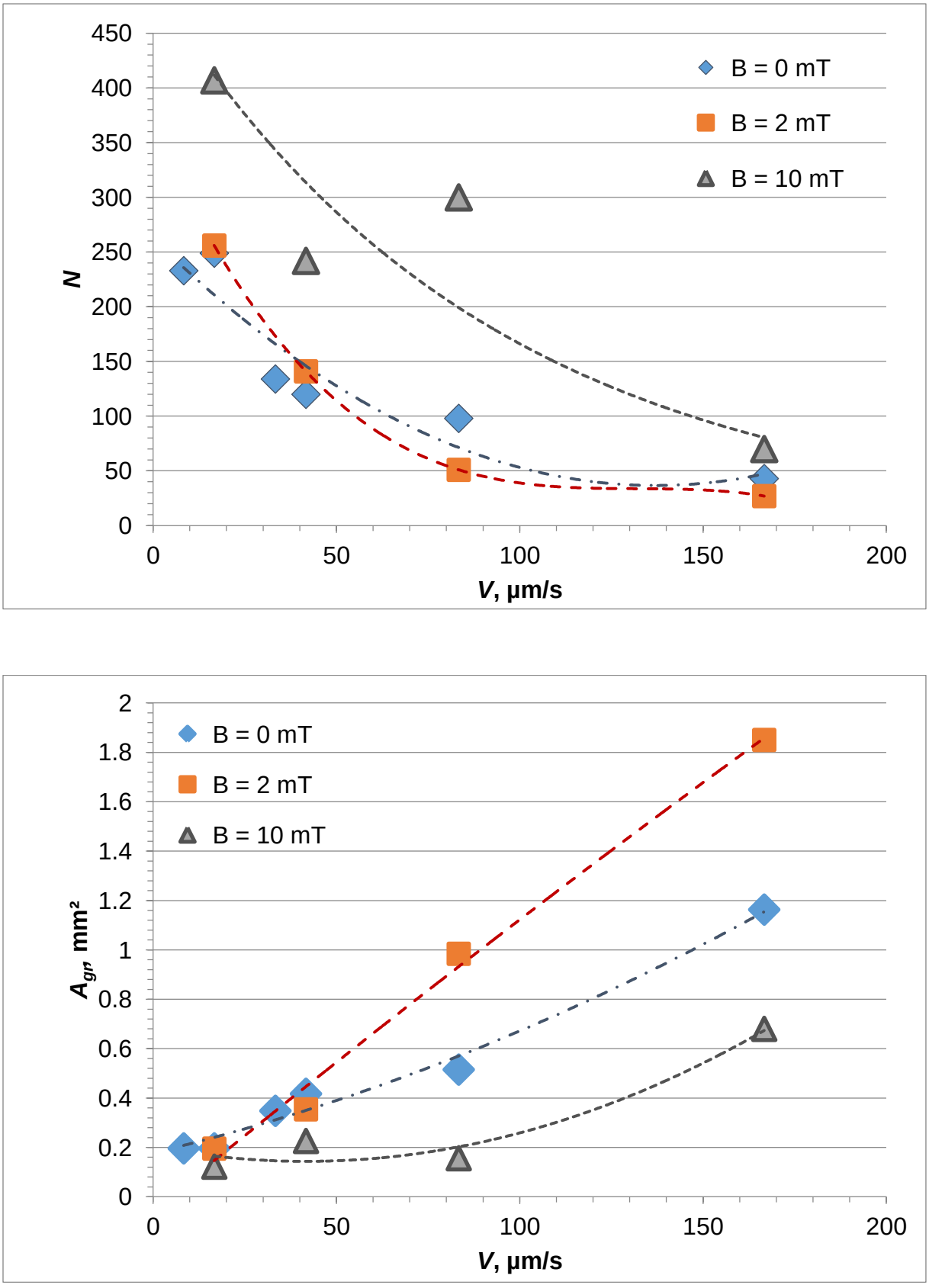

Fig. 5: Average number of grains N (top) and average grain size A_{gr} (bottom) for different solidification velocities V and different magnetic induction B with trend lines for better allocation

Figure 6

a)

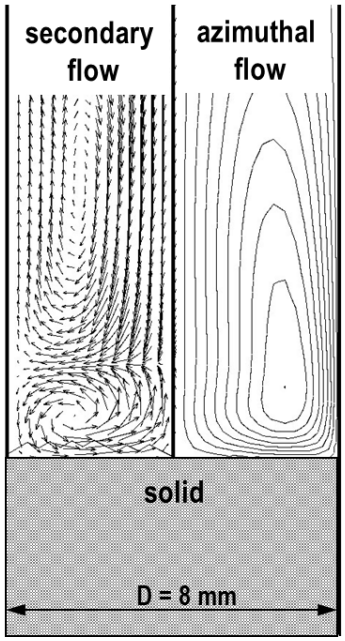
secondary flow
azimuthal flow
solid
D = 8 mm

b)

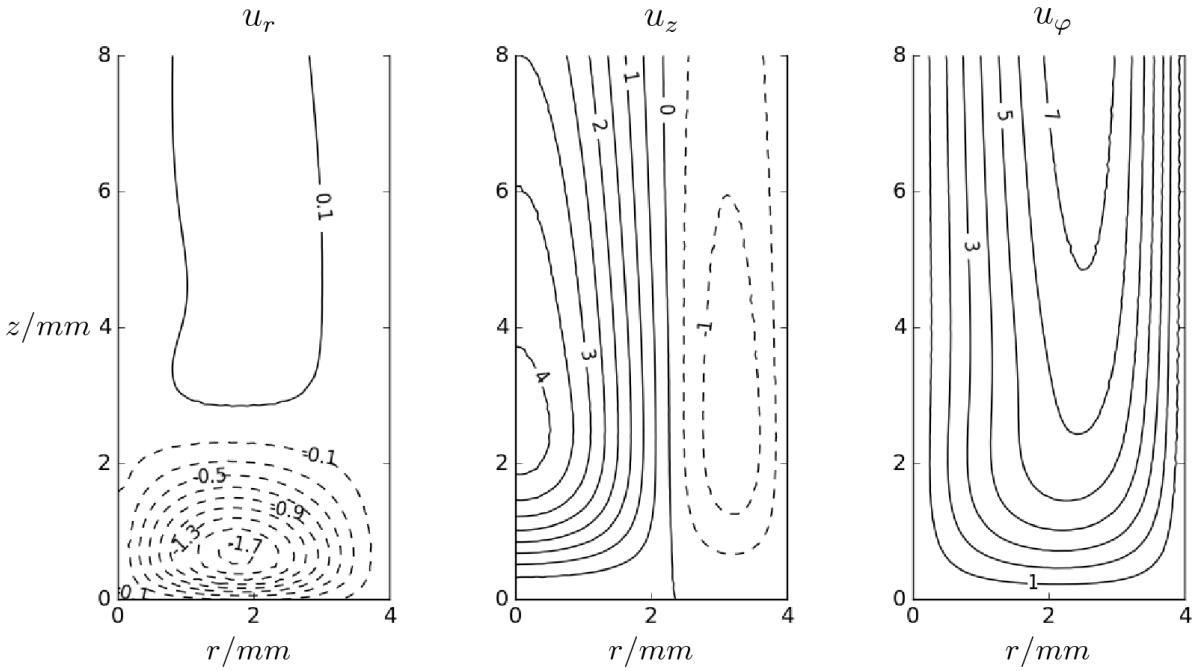
u_r
u_z
u_φ
z/mm
r/mm
r/mm
r/mm
0.1
-0.1
-0.5
-0.9
-1.3
-1.7
1
0
-1
2
3
4
5
7

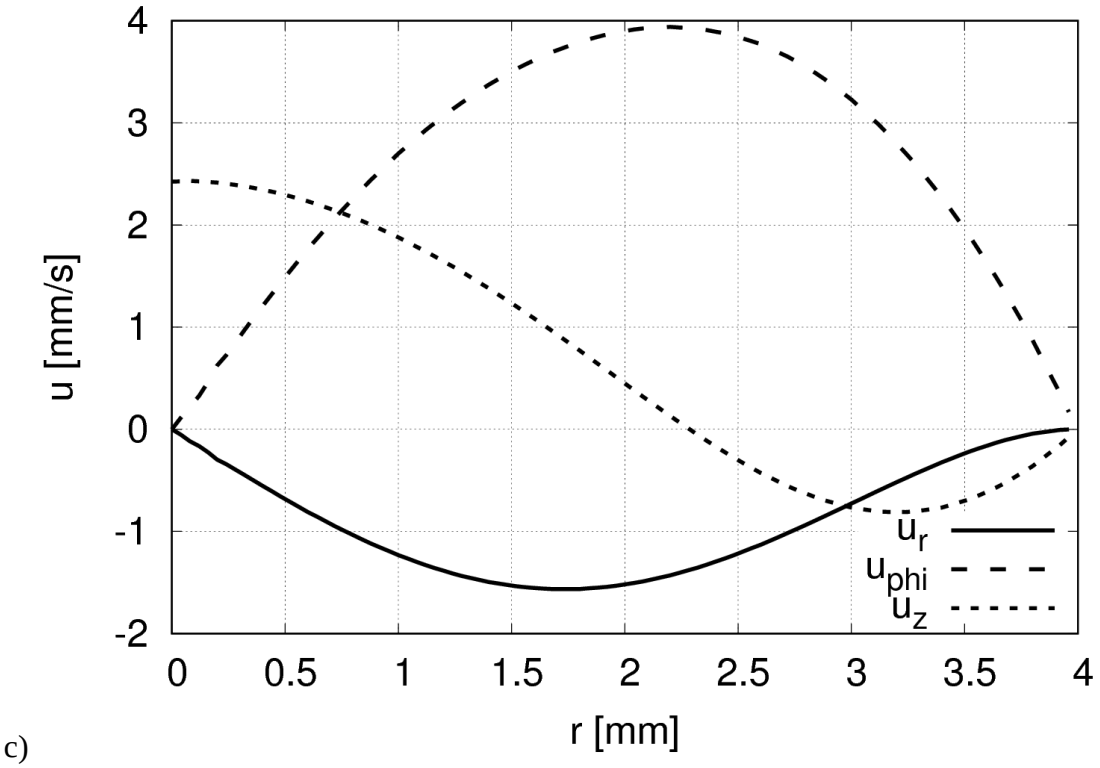

c) d)

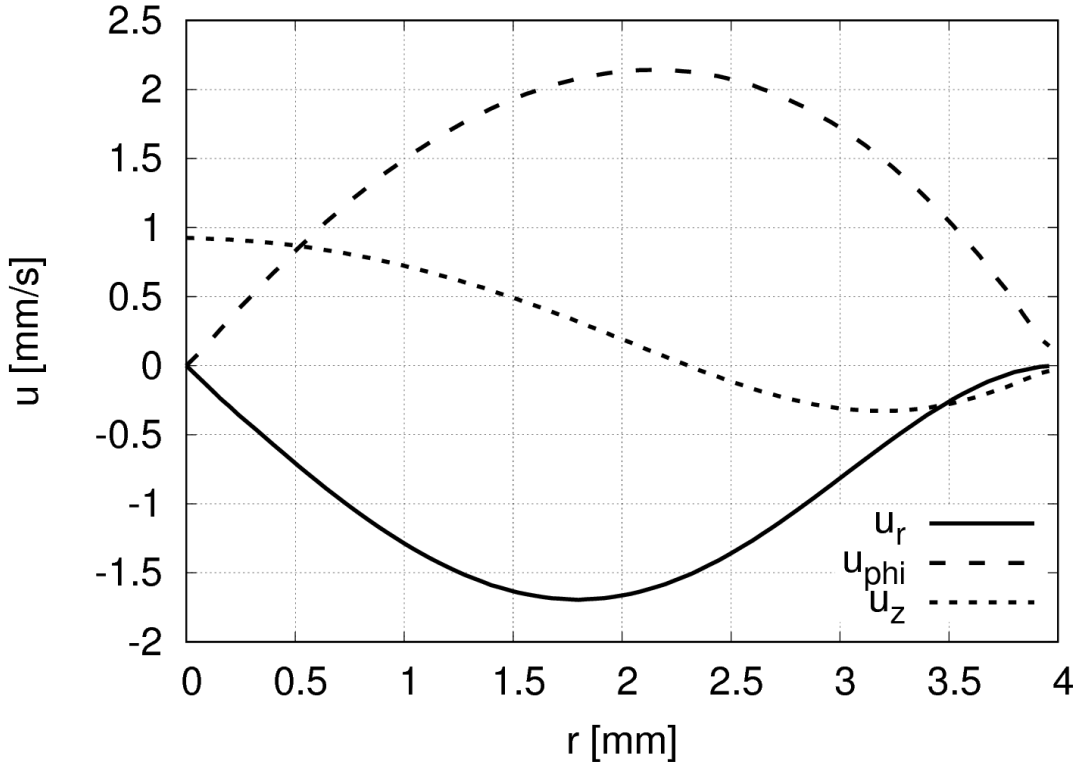

Fig. 6: a) Sketch of the flow structures induced by an RMF consisting of a primary azimuthal flow and a secondary meridional flow, b) calculated distributions of all velocity components for a magnetic induction of B = 2 mT, and velocity profiles at distances from the bottom of c) 1 mm and d) 0.5 mm.

Figure 7

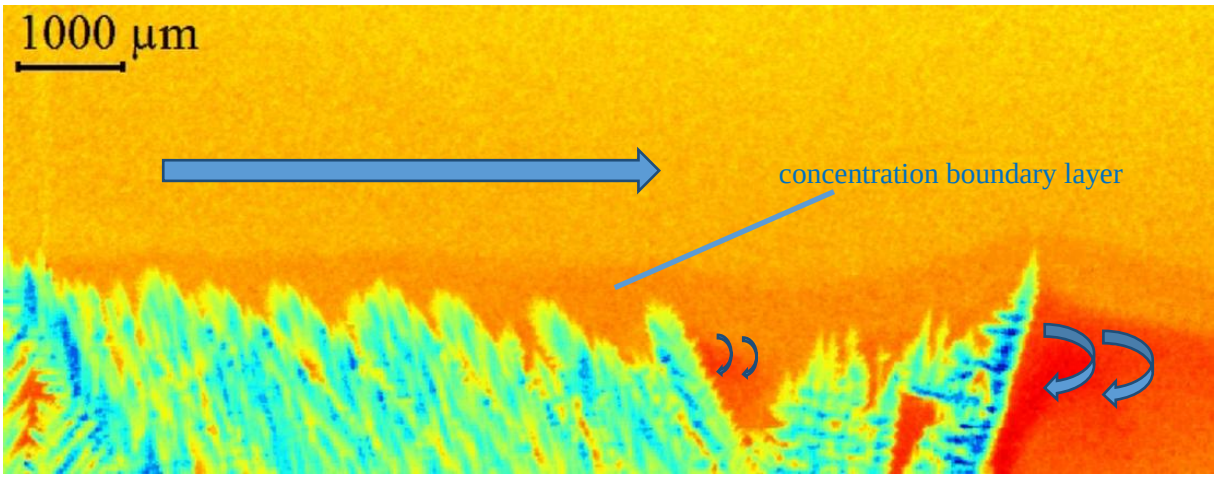

Fig. 7: X-ray visualization of directional solidification in Ga-25wt%In alloy under the effect of an incident lateral melt flow produced by a magnetic pump [34]. The colors represent the local composition of both the solid and the liquid phase (blue – In dendrites, red – Ga-rich liquid). The blue arrows mark the flow direction.

Figure 8

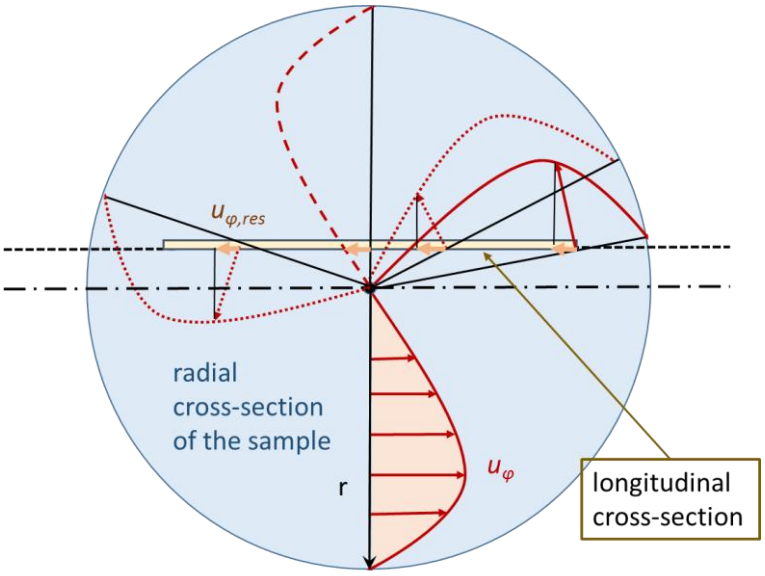

Fig. 8: Location of the longitudinal cross-section in the solidified Al-10wt%Cu sample with schematic azimuthal flow field u_φ in a horizontal plane and the lateral component $u_{\varphi,res}$ in the longitudinal cross-section

Graphical Abstract

Reduced grain refinement in directionally solidified refined Al-10wt%Cu alloy (V = 83 µm/s, G = 10 K/mm) in a rotating magnetic field (f = 50 Hz, B) due to laminar melt flow

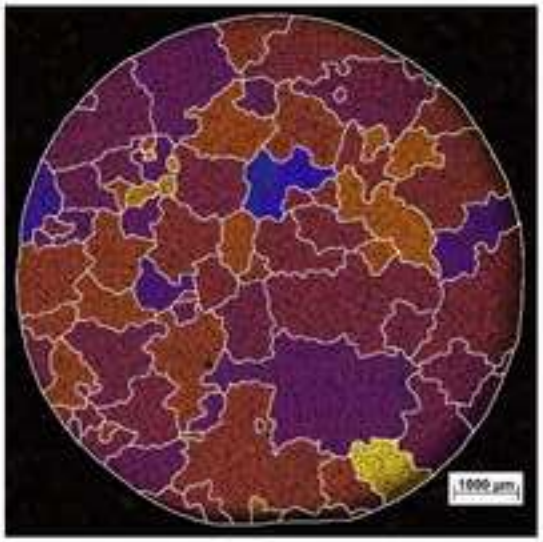

No forced melt flow (B = 0 mT)

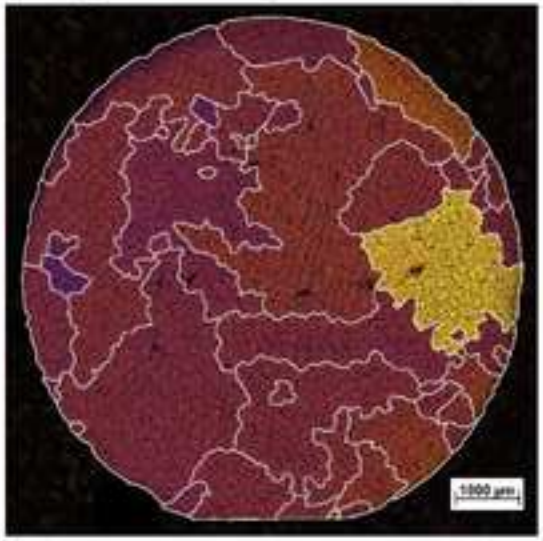

Laminar melt flow (B = 2 mT)

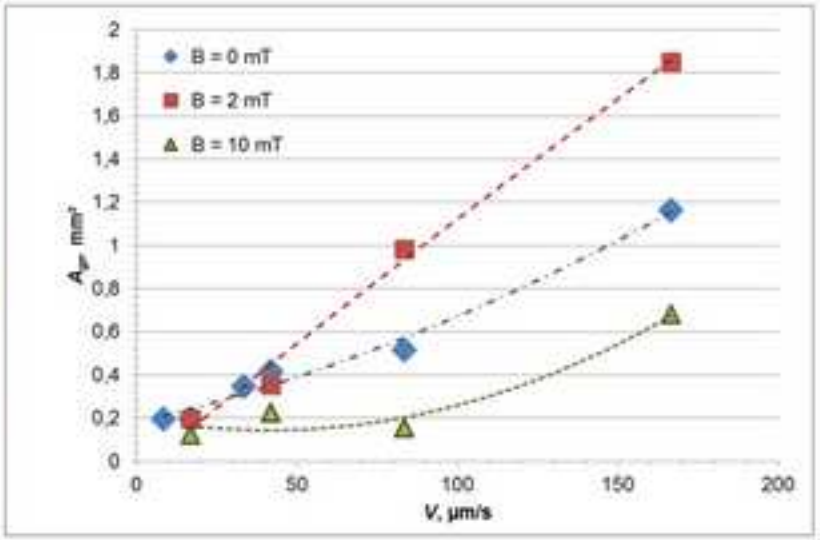

Average grain size A_{gr} for different flow intensities